Industrial Crops & Products 237 (2025) 122221

Contents lists available at ScienceDirect

Industrial Crops & Products

journal homepage: www.elsevier.com/locate/indcrop

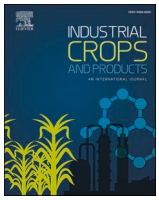

Catalytic and biocatalytic cascade conversion of giant reed and cardoon residues to glucose, levulinic acid, and long-chain fatty acid methyl esters

Antonio Caporusso [a,*,1], Nicola Di Fidio [b,1,*], Federico Liuzzi [a], Egidio Viola [a], Isabella De Bari [a]

[a] Italian National Agency for New Technologies, Energy and Sustainable Economic Development (ENEA), Laboratory for Processes and Technologies for Biorefineries and Green Chemistry, ENEA C.R. Trisaia S.S. 106 Jonica, Rotondella, MT 75026, Italy
[b] Department of Biosciences, Biotechnology and Environment, University of Bari "Aldo Moro", Via E. Orabona, 4, Bari 70125, Italy

ARTICLE INFO

Keywords:
Giant reed
Cardoon
Single cell oil
Fatty acids methyl esters
Levulinic acid
Biorefinery

ABSTRACT

Giant reed was hydrolysed by the green salt $FeCl_3$ under microwave irradiation. Differently, cardoon residues were pretreated by steam explosion and hydrolysed by the same catalyst. Each pretreatment showed efficient biomass fractionation, with xylan hydrolysis reaching 99 mol% for giant reed and 70 mol% for cardoon. Then, glucose yields of 55 and 30 mol% were obtained for giant reed and cardoon, respectively, under mild reaction conditions (34 min, 150 °C, biomass loading 9 wt%, $FeCl_3$ 2.7 wt%). Sugars-rich hydrolysates were fermented by the yeasts *L. starkeyi* and *L. tetrasporus* to produce triglycerides. *L. starkeyi* achieved a lipid yield of 13.5 wt% from giant reed hydrolysate and 14.2 wt% from cardoon hydrolysate. *L. tetrasporus* reached a lipid yield of 16.0 and 17.6 wt% from giant reed and cardoon hydrolysate, respectively. Moreover, both yeasts were able to convert cardoon hemicellulose into triglycerides, reaching at pH 5.5 a lipid yield of 13.9 wt% (*L. starkeyi*) and 19.4 wt% (*L. tetrasporus*). These oils were converted to long-chain fatty acids methyl esters. The final valorisation of unconverted glucan in solid residues resulted in the $FeCl_3$-catalysed production of levulinic acid and formic acid to close the biorefinery cycle of both biomasses.

1. Introduction

Replacing fossil-based chemicals, materials, and fuels with bio-based ones is one of the United Nations' sustainable development goals (Kobayashi and Nakajima, 2021). The European Union has set a target of 14 % for the share of renewable energy (biofuels, hydrogen, biomethane) used in transport by 2030, with a double counting for advanced biofuels. Although biofuels production has suffered a decline for the first time in recent years, due to the COVID-19 emergency, the global production of biofuels is expected to reach 3.2 million barrels of oil equivalent per day by 2025 (Keramidas et al., 2021).

Traditional biodiesel is produced on an industrial scale starting from vegetable oils obtained from oleaginous crops, such as palm oil and soybean oils, mainly sourced from Asia and South America. The intensive cultivation of oilseed crops has led to deforestation, loss of natural habitat and higher CO_2 emissions than the fossil diesel it replaces (Taheripour et al., 2022). However, the food application of these oilseed crops has raised an ethical debate on the right use of these renewable resources and the competition between the energy industry and the food chain. For all these regions, oilseed crops such as palm, soybean, and rapeseed have been discouraged, in RED III, for biofuel synthesis.

An innovative and promising solution is represented by Single Cell Oils (SCOs) produced from oleaginous yeasts. Oleaginous yeasts can accumulate up to 70 % of their dry cell weight in lipids and can store them in intracellular lipid bodies in the form of triglycerides.

The typical lipids profile of SCOs is very similar to the main vegetable oils (Kumar et al., 2025). Moreover, SCOs represent a source of platform chemicals for several biobased products, such as surfactants, lubricants, food additives, plastics, paints, detergents, and biofuels (Caporusso et al., 2025; Pizzimenti et al., 2022).

The main species of oleaginous yeasts belong to the genera *Yarrowia, Cryptococcus, Lipomyces, Rhodosporidium,* and *Rhodotorula*. Among these, the genera *Lipomyces* is considered very interesting due to their metabolic performances, such as the use of both glucose and xylose as a carbon source, high lipid yields, the low consumption of its intracellular lipids, the capability to grow in simple media and the good tolerance to

* Corresponding authors.
E-mail addresses: antonio.caporusso@enea.it (A. Caporusso), nicola.difidio@uniba.it (N. Di Fidio).
[1] Co-first authors: A.C. and N.D.F. contributed equally to the manuscript

https://doi.org/10.1016/j.indcrop.2025.122221
Received 18 July 2025; Received in revised form 15 October 2025; Accepted 30 October 2025
Available online 6 November 2025

inhibitory compounds, such as aldehydes, alcohols, and organic acids (Szczepańska et al., 2022).

Nevertheless, the actual high prices of commercial media significantly restrict the economic competitiveness of SCO compared to vegetable oil (Gallego-García et al., 2022). Conversely, lignocellulosic raw materials derived from crop residues are more cost-effective (Caporusso et al., 2023b).

Lignocellulosic biomasses represent the most abundant and important renewable resources for the sustainable production of bioproducts (Madadi et al., 2025). Biorefining of lignocellulosic biomass to give products and energy represents a sustainable way to favour the decarbonisation of industrial activities and to face environmental issues (Tan et al., 2025).

Giant reed and cardoon represent two promising starting feedstocks to produce second-generation sugars, which are the ideal carbon source for the production of SCO (Kumar et al., 2025). Giant reed (*Arundo donax* L.) is a perennial herbaceous rhizomatous plant characterised by high structural carbohydrate content, up to 60 wt%, high production yield (about 35–45 tons/hectare/year), and the ability to grow in a wide range of climatic habitats, including marginal quality lands with low input requirements (Ortega et al., 2024). Cardoon (*Cynara cardunculus* L.) is a perennial herbaceous plant belonging to the *Asteraceae* family (Mandim et al., 2023). Cardoon cultivation is spread over 2000–3000 ha in marginal lands of different Mediterranean countries, such as Spain, Italy, Greece, and France. The yield ranges from 9 to 26 tons per hectare of dry biomass (Ortega et al., 2024), influenced by annual precipitation and the genotype utilised (Mandim et al., 2023). In Italy, cardoon cultivation is located in Sardinia, with approximately 500 ha, thanks to the Novamont S.p.A. biorefinery, where the company has created a multi-product biorefinery using cardoon seed oil as a platform for bio-based plastic (De Bari et al., 2020). Lignocellulosic residues represent approximately 70–80 wt% of the entire cardoon plant, and their high holocellulose content (50–60 wt%) makes cardoon an attractive feedstock for SCOs production.

The technologies and catalytic approaches utilised in biomass pretreatment, hydrolysis, and subsequent downstream processes have a significant impact on the economic feasibility of biorefinery systems. For the hydrolysis phase, the homogeneous catalyst $FeCl_3$ offers notable benefits over traditional strong inorganic acids. These advantages include reduced reactor corrosion, cost-effectiveness, straightforward recovery through precipitation, high efficiency under mild conditions, energy conservation, and favourable selectivity (Di Fidio et al., 2021).

Additionally, research indicates that certain metal ions used during biomass pretreatment or cellulose hydrolysis, including Fe^{3+}, serve as essential nutrients for various salt-tolerant microorganisms involved in fermenting second-generation sugars (Wang et al., 2012).

The objective of this study was the investigation of the microwave-assisted $FeCl_3$-catalysed hydrolysis of giant reed and cardoon cellulose to give glucose-rich hydrolysate. The latter was used as substrate for the bioconversion into SCO, namely a promising platform chemical, by the two oleaginous yeasts *L. starkeyi* DSM 70296 and *L. tetrasporus* DSM 70315. Then, SCO was converted into long-chain fatty acid methyl esters, representing a new generation biodiesel.

The giant reed cellulose-rich residue was obtained after the selective hemicellulose hydrolysis by microwave-assisted $FeCl_3$-catalysed treatment (Di Fidio et al., 2020a), whereas the cardoon cellulose-rich one was recovered at the end of the steam-explosion pretreatment (Caporusso et al., 2021).

To enhance the environmental, technical, and economic sustainability of biorefineries utilising lignocellulosic biomass, cellulose hydrolysis was investigated under relatively mild reaction conditions. This approach integrates the use of microwaves, which provide a more energy-efficient and cost-effective heating method, with homogeneous catalysis employing the low-cost inorganic salt $FeCl_3$. Bioconversion tests were carried out with the two yeasts on the cellulose and hemicellulose hydrolysed fractions in order to increase the process sustainability. Finally, the residual cellulose contained in the final solid was converted to added-value bio-products levulinic and formic acids by adopting the same chemical catalytic approach under different reaction conditions.

At the end of the entire cascade process, a lignin-rich solid residue was obtained, representing a promising renewable material for the production of hydrochar, pyrochar, or microporous activated carbons for the adsorption of CO_2 and/or organic pollutants (Di Fidio et al., 2020a).

From a circular economy and green chemistry perspective, all lignocellulosic fractions of the starting feedstocks have been valorised through a process designed without significant waste or outflows.

2. Materials and methods

2.1. Feedstock and reagents

Giant reed (*Arundo donax* L.) biomass was harvested in Northern Italy (province of Vercelli). The feedstock was composed of culms and leaves, which were ground into 1.0 mm average size fibres, dried at 105 °C in an oven until a constant weight, and stored in a desiccator until their use. Cardoon (*Cynara cardunculus* L.) was sourced from the experimental fields of Matrica Biorefinery located in Porto Torres (Sardinia) and was pretreated using the steam explosion batch technology (Staketech, 10 L reactor) of ENEA Trisaia.

The analysis of the chemical composition of raw giant reed and cardoon, pretreated biomasses, and all the process solid residues was evaluated as previously described (Caporusso et al., 2023a; Di Fidio et al., 2019).

All reagents were of analytical purity grade and purchased from Merck company (Saint Louis, MO, USA).

2.2. Microwave-assisted pretreatment of giant reed

Microwave-assisted $FeCl_3$-catalysed pretreatment of giant reed was performed under the reaction conditions optimised in a previous work (Di Fidio et al., 2020a). The process was carried out in a multimodal microwave reactor CEM MARS 6. Giant reed (3 g) was charged in the microwave reactor (80 mL) containing water (30 mL) and $FeCl_3{\cdot}6\ H_2O$ (0.84 g) according to the solid loading of 9 wt% and the catalyst concentration of 1.6 wt%. The system was stirred for 5 min and then heated in the microwave reactor at 150 °C for 5 min under magnetic stirring. At the end of the reaction, the vessel was rapidly cooled to room temperature through an external air flow. The solid fraction was recovered by filtration under vacuum, dried at 105 °C in an oven until reaching a constant weight, and stored in a desiccator until its use.

The biomass loading (BL) was calculated as follows:

$$BL\ (wt\%) = m_b\ /\ (m_b + m_{water}) \times 100 \quad (1)$$

where m_b is the amount of the biomass in grams.

The catalyst amount was calculated according to the following equation:

$$FeCl_3(wt\%) = \left(0.6 \times m_{FeCl_3*6H_2O}\right) / \left(m_{H_2O} + m_{FeCl_3*6H_2O}\right) \times 100 \quad (2)$$

where 0.6 is the ratio between the molecular weight values of ferric chloride and ferric chloride hexahydrate, $m_{FeCl3*H2O}$ and m_{H2O} are the amounts in grams of ferric chloride hexahydrate and water, respectively.

2.3. Steam explosion pretreatment of cardoon

The steam explosion pretreatment of cardoon residue was carried out at 195 °C for 7.5 min according to process conditions previously optimised (Caporusso et al., 2021).

Prior to the pretreatment, biomass was crumbled to a particle size in the range 1.7–5.6 mm, and it was soaked in a dilute H_2SO_4 solution

(0.03 M) for 10 min. The resulting acid loading was 0.6 wt%. The pretreated products consisted of a cellulose-rich solid fraction and a xylose-rich liquid fraction, deriving from hemicellulose depolymerisation.

2.4. Two-stage microwave-assisted conversion of cellulose to glucose and levulinic acid

Two-stage microwave-assisted $FeCl_3$-catalysed conversion of the cellulose fraction of both giant reed and cardoon to glucose and levulinic acid was performed by using the same microwave reactor described in Section 2.2. In the first stage, the conversion of cellulose to glucose was performed under previously optimised reaction conditions. In order to completely exploit the carbohydrates of biomass, in the second stage, the remaining cellulose in the solid residue was converted to levulinic and formic acids by using the previously optimised reaction conditions reported by Di Fidio et al. (2020a).

Regarding the glucose production, the substrate loading of 9 wt% (3 g cellulose-rich residue in 30 mL H_2O), reaction time of 34 min, temperature of 155 °C and $FeCl_3$ concentration of 2.7 wt% were adopted for both the pretreated biomasses. At the end of the reaction, the liquid fraction, corresponding to the glucose-rich hydrolysate, was recovered by filtration and analysed by HPLC. The solid residue was washed with deionised water, dried at 105 °C in an oven until constant weight, and then stored in a desiccator until its use.

Regarding the levulinic acid production, the substrate loading was 9 wt%, the reaction time was 15 min, the $FeCl_3$ amount was 2.4 wt%, and the temperature was 190 °C. The liquid-to-solid separation was performed by filtration, and the liquid fraction was analysed by HPLC.

The glucose yield was calculated as follows:

$$\text{Glucose yield (mol\%)} = [(m_g \times 0.90) / (m_b \times G_b/100)] \times 100 \quad (3)$$

where m_g is the glucose amount (g), 0.90 is the ratio between the molecular weight values of the glucan monomer and the glucose, m_b is the mass (g) of the substrate, G_b is the percentage of glucan in the dry pretreated biomass (wt%).

The LA yield (mol%) with respect to the glucan moles of the solid residue, obtained from the chemical hydrolysis of the cellulose fraction of the pretreated biomass, was calculated as follows:

$$\text{Levulinic yield (mol\%)} = [(m_{LA} \times 1.40) / (m_r \times G_r/100)] \times 100 \quad (4)$$

where m_{LA} is the LA amount (g), 1.40 is the ratio between the molecular weight values of the glucan monomer and the LA, m_r is the mass (g) of the solid residue employed as the substrate, G_r is the percentage of glucan in the dry solid residue (wt%).

2.5. High performance liquid chromatography analysis

Sugars (glucose, xylose) were quantified by HPIC (High Performance Ionic Chromatography) Dionex ICS-2500 System equipped with a Nucleogel Ion 300 OA operating at 40 °C with 10 mM H_2SO_4 solution as mobile-phase (0.4 mL/min). The detector was a Shodex RI-101 Refractive Index. Organic acids (acetic acid, formic acid, levulinic acid) and furan-derivatives (5-hydroxymethylfurfural, furfural) were quantified by HPLC, an HP1100 system equipped with a Dionex AS1 column operating at 30 °C with Milli-Q Water/Acetonitrile as mobile-phase (0.7 mL/min) and a diode array detector. Both standards and samples were analysed three times, and the experimental error resulted within 4 %.

2.6. Yeast strain and inoculum preparation

The oleaginous yeast strains *Lipomyces starkeyi* DSM 70296 and *Lipomyces tetrasporus* DSM 70314 were provided by DSMZ (Germany). They were stored at 4 °C and propagated every 4 weeks on a solid medium (glucose 20 g/L, peptone 10 g/L, yeast extract 10 g/L, agar 20 g/L, pH 6.0). The cultivation protocol was already described in a previous work (Caporusso et al., 2021). A calculated volume of the preculture was added to the fermentation medium in order to reach the inoculum concentration of 3.0 g/L dry cell weight (DCW).

2.7. Single cell oil production

Batch cultures (50 mL) were performed in 250 mL Erlenmeyer flasks at 30 °C. Fermentations were extended until the almost complete depletion of sugars in the medium. Each test was replicated three times. The initial pH was adjusted to 5.5 or 6.5 with an acid or basic solution, according to the experimental set-up. The agitation was guaranteed by a rotary shaker set at 180 rpm.

Giant reed and cardoon hydrolysates were supplemented with the following nutrients: $MgSO_4 \cdot 7\ H_2O$ 1.5 g/L, phosphate buffer (KH_2PO_4 7 g/L, $Na_2HPO_4 \cdot 2\ H_2O$ 5 g/L), $FeSO_4 \cdot 7\ H_2O$ 0.08 g/L. A proper amount of yeast extract was also added to reach the carbon to nitrogen weight ratio of 40 g/g, useful to ensure biomass growth and lipid synthesis. Then the lignocellulosic hydrolysates were sterilised by microfiltration (0.22 μm).

During batch cultivation, yeast growth, sugars concentration, and intracellular lipid content were monitored by DCW quantification, HPLC analysis, and lipids extraction, respectively. Two samples of 1 mL were withdrawn every 24 h and centrifuged to separate cells from the culture medium. Cells were washed three times with deionised water and oven-dried at 70 °C in order to obtain the DCW concentration. The liquid fraction was used for quantifying the sugars concentration by HPLC.

2.8. Single cell oil extraction

During and after fermentation processes, yeast cells were harvested by centrifugation, washed twice with distilled water, lyophilised and stored in a desiccator until the triglycerides extraction. The latter was performed according to our previous work (Caporusso et al., 2021). Briefly, lyophilised cells (200–400 mg) were suspended in 10 mL of 1 M HCl solution for 2 h at 60 °C under conventional heating (oil bath) to promote the cell membrane lysis. Then, 20 mL of 2-methyltetrahydrofuran (2-MeTHF) was added to the acid-hydrolysed cells suspension, and the obtained biphasic system was stirred at room temperature for 1 h. After that, the separation of different phases was obtained, and the organic phase containing lipids was transferred into a glass vial. Then the drying of lipids was performed by using a rotary evaporator under vacuum at 40 °C. Finally, the total amount of oil was gravimetrically quantified.

The amount of yeast biomass produced at the end of batch cultures, the amount of extracted lipids, the glucose and xylose consumption and the incubation time required for obtaining the complete depletion of sugars were used to calculate the intracellular lipid content (wt%), the lipid production (g/L), the lipid yield (wt%) and the process productivity (g/L/d) according to the following equations:

$$\text{Lipid content (wt\%)} = (m_L / m_{cells}) \times 100 \quad (5)$$

$$\text{Lipid production (g/L)} = (m_L / m_{cells}) \times c_{cells} \quad (6)$$

$$\text{Lipid yield (wt\%)} = (c_L / c_s) \times 100 \quad (7)$$

$$\text{Productivity (g/L/d)} = (c_L / t)) \quad (8)$$

where $_{mL}$ is the amount of the lipids in g, m_{cells} is the lyophilised yeast biomass in g, c_{cells} is the yeast biomass concentration (g/L) obtained at the end of the batch culture, c_L is the production of lipids in g/L, c_s is the concentration (g/L) of consumed sugars (glucose and xylose), and t is the fermentation time in days.

2.9. Synthesis and analysis of long-chain fatty acids methyl esters from SCO

The transesterification of SCOs to fatty acids methyl esters (FAMEs) and the GC-FID analysis were performed according to previous studies (Caporusso et al., 2021). GC analyses were carried out by an Agilent GC7890A gas chromatograph, equipped with a HP-INNOWax 19091N-213 capillary column (30 m × 0.32 mm × 0.50 μm) and a flame ionisation detector. The oven temperature was programmed at 80 °C for 11 min, from 80 °C to 180 °C at a rate of 20 °C/min and held at 180 °C for 22 min. Helium was the carrier gas at 80 kPa, and the split ratio was 1:19 v/v.

3. Results and discussion

3.1. Chemical composition of raw and pretreated giant reed and cardoon stalks

Biomasses were characterised according to the National Renewable Energy Laboratory (NREL) protocols (Sluiter et al., 2008a, 2008b, 2004a, 2004b). The chemical composition of raw and pretreated giant reed and cardoon stalks (defatted cardoon) was reported in Table 1.

The compositional results for the raw giant reed were comparable to those reported by Madian et al. (2022) with an overall holocellulose content of 56 wt%. In accordance with a previously reported study (Lemões et al., 2018), the cellulose content (36 wt%) was comparatively higher than the hemicellulose content (20 wt%). Similarly, cardoon showed a cellulose content (38 wt%) higher than the hemicellulose one (17 wt%), in agreement with the chemical composition reported by Fernandes et al. (2018).

For giant reed, the microwave-assisted $FeCl_3$-catalysed pretreatment (9 wt% biomass loading, 1.6 wt% $FeCl_3$, 150 °C, 5 min) allowed the complete removal of xylan and the obtaining of a cellulose-rich solid residue containing 50 wt% glucan. Similarly, for cardoon stalks, H_2SO_4-catalysed steam explosion pretreatment (195 °C, 7.5 min, 20 bar, 0.6 wt % H_2SO_4) ensured the almost complete removal of xylan, and a cellulose-rich solid residue was obtained containing 56 wt% glucan and around 3.7 wt% xylan. For both types of pretreatments, the reaction conditions were accurately selected to minimise the production of furanic derivatives, such as furfural and 5-hydroxymethylfurfural, deriving from the dehydration reaction of xylose. Moreover, the two pretreated solids were characterised by a similar lignin content of around 30 wt%.

Given their similar chemical compositions, the same reaction conditions were applied to both pretreated biomasses for cellulose hydrolysis to produce glucose: substrate loading of 9 wt%, reaction time of 34 min, 2.7 wt% $FeCl_3$, temperature of 155 °C and microwave heating.

Table 1
Chemical composition (wt% on dry matter) of unpretreated biomasses, acid-pretreated giant reed, and steam-exploded cardoon stalks.

Fraction (wt%)	Raw giant reed	Raw cardoon	Pretreated giant reed	Pretreated cardoon
Glucan	36.3 ± 0.4	37.6 ± 0.3	50.0 ± 1.7	56.2 ± 0.3
Xylan	17.3 ± 0.2	12.4 ± 0.4	n.d.	3.7 ± 0.1
Arabinan	1.9 ± 0.1	4.4 ± 0.1	n.d.	n.d.
Mannan	0.6 ± 0.0	n.d.	n.d.	n.d.
Acetyl groups	3.6 ± 0.1	4.0 ± 0.2	0.6 ± 0.0	2.1 ± 0.1
Extractives	15.4 ± 0.8	7.6 ± 0.1	11.6 ± 3.2	0
Ash	2.0 ± 0.1	8.8 ± 0.3	3.0 ± 0.2	3.4 ± 0.3
Acid-soluble lignin	0.9 ± 0.1	1.2 ± 0.0	0.4 ± 0.2	0.3 ± 0.1
Acid-insoluble lignin	22.0 ± 0.3	17.5 ± 0.4	34.4 ± 1.1	31.4 ± 0.5
Other components	-	6.5 ± 1.8	-	2.9 ± 1.4

3.2. Chemical composition of giant reed and cardoon stalks hydrolysates

The chemical composition of the sugars-rich hydrolysates obtained from the microwave-assisted $FeCl_3$-catalysed hydrolysis of pretreated giant reed and cardoon was reported in Table 2.

Hydrolysates obtained from the cellulose fraction of pretreated giant reed and cardoon were characterised by a similar reducing-sugars content of around 20 g/L. The first one contained 22.2 g/L of glucose, while the second one contained 18.1 g/L as the sum of glucose and xylose. In terms of by-product concentration, the giant reed hydrolysate exhibited a higher content of organic acids (4.1 g/L formic acid and 4.2 g/L levulinic acid) and 5-HMF (1.3 g/L) than the cardoon hydrolysate. Conversely, the latter was characterised by a higher concentration of furfural (1.5 g/L) deriving from the hemicellulose fraction, which was absent in the giant reed substrate. Overall, giant reed and cardoon hydrolysates contained 1.3 and 1.7 g/L of furanic derivatives (HMF and furfural), respectively.

The biological conversion of several substrates to microbial oils by *L. starkeyi* has been extensively studied (Zhang et al., 2022). In the present paper, for the first time, the fermentation of glucose-rich hydrolysates obtained from the $FeCl_3$-catalysed hydrolysis of giant reed and cardoon was compared. This innovative chemical catalytic approach can overcome some drawbacks typical of enzymatic catalysis, widely used for the hydrolysis of lignocellulosic biomasses, such as the high cost of the catalyst and the very long reaction time (Zhang et al., 2022). In fact, the glucose productivity was around 40 and 30 g/L/h for giant reed and cardoon hydrolysis, respectively. These values are around 100 times higher than those achieved by enzymatic hydrolysis for the same type of pretreated biomass as well as for other types of pretreated lignocellulosic biomasses, as reported in previous studies (Caporusso et al., 2021; D'Orsi et al., 2023; Di Fidio et al., 2021) (Table 3).

At the same time, homogeneous acid catalysis is characterised by a lower selectivity towards glucose and xylose, thus requiring a tailored optimisation of the main reaction parameters aimed at minimising the formation of by-products. In fact, on one hand, the undetoxified giant reed hydrolysate was suitable for yeasts growth. On the other hand, after a preliminary test, *L. starkeyi* was found to be not suited for growing on cardoon hydrolysate due to the presence of a relatively high concentration of furfural (1.5 g/L, Table 2), which represents the main inhibitor of the yeast growth, as previously demonstrated (Di Fidio et al., 2021). For this reason, furfural was removed by vacuum evaporation and the obtained concentrated hydrolysate, containing 32.2 g/L glucose, 4.0 g/L xylose, 0.4 g/L 5-HMF, 3.6 g/L levulinic acid, 2.6 g/L formic acid, was diluted 1:1 v/v with distilled water in order to restore the initial concentration of sugars and other hydrolysate's components and make it comparable with respect to the giant reed hydrolysate. After the dilution, the fermentation of the hydrolysate (16.2 g/L glucose, 2.1 g/L xylose, 0.2 g/L 5-HMF, 1.8 g/L levulinic acid, 1.2 g/L formic acid) was successfully carried out and the results were compared with those obtained by fermenting the glucose-rich hydrolysate from giant reed. Finally, the liquid fraction deriving from the acid-catalysed steam explosion pretreatment of cardoon stalks was also tested as a culture medium in the fermentation process by *L. starkeyi* and *L. tetrasporus* in order to exploit this process side-stream in line with the principles of Green Chemistry and sustainability goals. In fact, this xylose-rich fraction contained around 17 g/L of reducing sugars and a relatively low concentration of furanic derivatives (0.7 g/L as the sum of furfural and HMF), making it a promising carbon source for xylose-consuming yeasts. Similarly, the xylose-rich hydrolysate deriving from the $FeCl_3$-catalysed pretreatment of giant reed under the optimised reaction conditions adopted in the present study was fermented by *L. starkeyi* in our previous work (Di Fidio et al., 2021).

Table 2
Chemical composition of glucose-rich hydrolysates obtained by the microwave-assisted $FeCl_3$-catalysed hydrolysis of giant reed and cardoon cellulose-rich residues, as well as the chemical composition of the xylose-rich hydrolysate obtained from each pretreatment step.

Type of hydrolysate	Glucose (g/L)	Xylose (g/L)	FA (g/L)	AA (g/L)	LA (g/L)	HMF (g/L)	FUR (g/L)
Giant reed cellulose	22.2	n.d.	4.1	n.d.	4.2	1.3	n.d.
Cardoon cellulose	16.1	2.0	1.3	0.8	1.8	0.2	1.5
Cardoon cellulose[a]	32.2	4.0	2.6	1.6	3.6	0.4	n.d.
Cardoon cellulose[b]	16.2	2.1	1.2	0.8	1.8	0.2	n.d.
Giant reed hemicellulose	5.6	19.4	0.5	2.2	n.d.	0.4	0.3
Cardoon hemicellulose	0.9	15.6	0.4	4.7	1.2	0.2	0.5

FA = formic acid; AA = acetic acid; LA = levulinic acid; HMF = 5-hydroxymethylfurfural; FUR = furfural; n.d. = not detected.
[a] hydrolysate after the selective removal of furfural by vacuum evaporation.
[b] hydrolysate after the selective removal of furfural by vacuum evaporation and dilution.

Table 3
An overview of the literature on saccharification efficiency, compared with the results reported in this work.

Biomass	Catalyst	Glucose production (g/L)	Glucose yield (mol %)	Glucose productivity (g/L/h)	Reaction time (h)	Reference
Giant reed	Cellic® CTec2	34.0	56	0.34	96.0	(Di Fidio et al., 2020b)
Rice husk	Crude cellulases of *A. niger*	1.8	-	0.07	25.0	(Efrinalia et al., 2022)
Cardoon stems	Cellic® CTec2	50.0	96	0.42	120.0	(Fabbrizi et al., 2022)
Cotton stalk	Cellulase of *T. reesei*	30.0	93	0.46	65.0	(Yildirim et al., 2023)
Cocoa pod husk	Cellic® CTec2	74.0	98	1.02	72.0	(Hernández-Mendoza et al., 2021)
Wheat straw	Cellic® CTec2	80.8	77	0.84	52.0	(Chen et al., 2021)
Giant reed	$FeCl_3$	22.2	59	40.0	0.6	This work
Cardoon stems	$FeCl_3$	16.1	30	30.0	0.6	This work

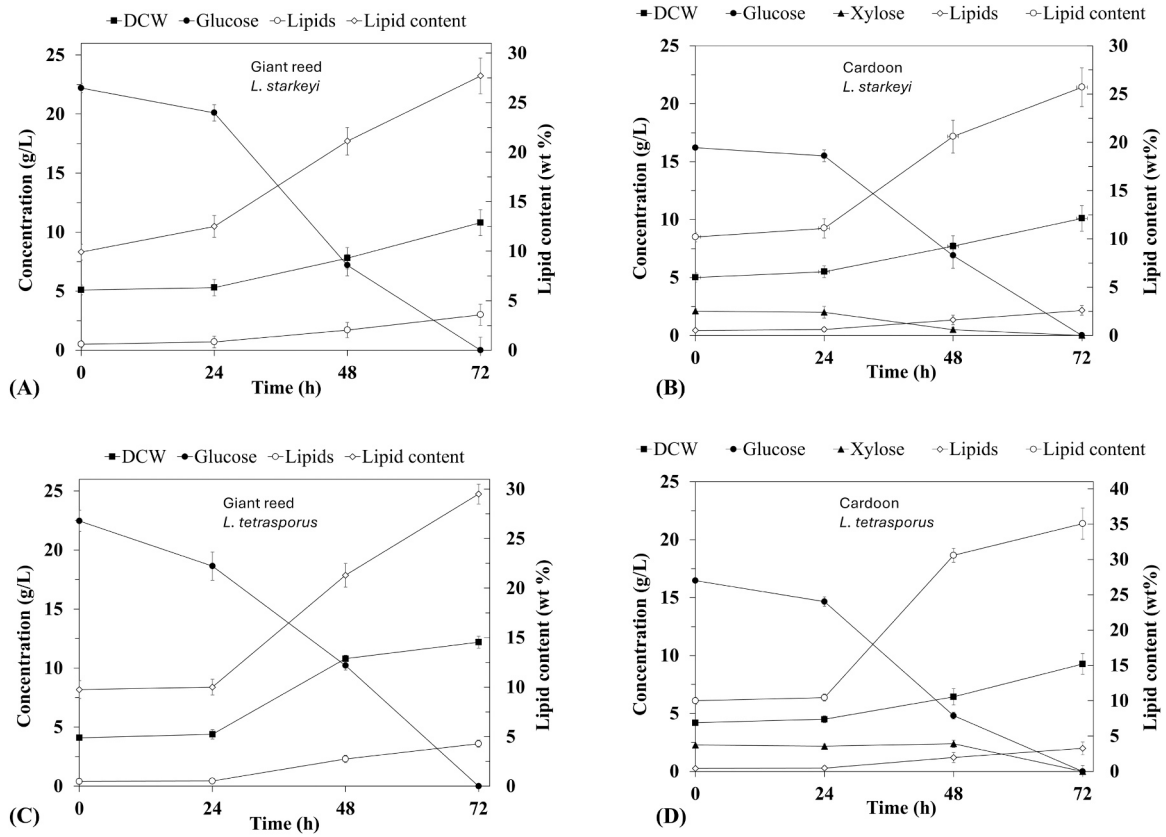

Fig. 1. Glucose concentration (g/L), xylose concentration (g/L), dry cell weight concentration (DCW, g/L), lipids concentration (g/L), and lipid content (wt%) as a function of reaction time during the giant reed hydrolysate fermentation (A, C) and cardoon hydrolysate (B, D) by *Lipomyces starkeyi* (A, B) and *L. tetrasporus* (C, D).

3.3. Bioconversion of giant reed and cardoon stalks cellulose hydrolysates to triglycerides

Fig. 1 shows the kinetics of the fermentation tests carried out on the undetoxified giant reed hydrolysate and the partially detoxified cardoon hydrolysate, respectively.

On both media, during the first 24 h, the growth phase was not observed for both yeasts due to their adaptation to the complex substrate, while from 24 to 72 h, the yeast growth significantly increased. In all the processes, the complete consumption of the carbon source was observed within 72 h.

L. tetrasporus was able to detoxify the medium in the first 24 h (Figs. 1C and 1D). In this phase, 5-hydroxymethylfurfural and furfural were metabolised, in agreement with a previous study (Caporusso et al., 2021). Moreover, in the first 24 h, the selective conversion of glucose was observed while xylose concentration remained almost constant according to the biochemical phenomenon of glucose repression typical of many yeasts and eukaryotic organisms (Mota et al., 2022). Differently, *L. starkeyi* was unable to metabolise 5-hydroxymethylfurfural and furfural, but biological detoxification still occurs as these molecules irreversibly bind to the yeast, causing cell death, according to the literature (Di Fidio et al., 2021). Although some cells died, a high-density inoculum (around 3.5 g/L) allowed the bioconversion of the hydrolysates. The first 24 h were characterised by a latency phase, followed by rapid yeast growth. The process was stopped at 72 h when the sugars concentration dropped to 0 g/L. For *L. starkeyi*, the net production of DCW was 5.7 and 5.1 g/L for giant reed and cardoon hydrolysate, respectively. It ranged from the starting value of 5 g/L to the final concentration of around 10 g/L.

The sugars content decreased from 24 to 72 h as a function of the increase in DCW concentration. In particular, in the case of the cardoon hydrolysate, the consumption of glucose and xylose was similar to that observed for the fermentation of the giant reed hydrolysate, confirming the ability of *L. starkeyi* to convert xylose into SCO.

Similarly, the net production of DCW for *L. tetrasporus* was 8.1 and 5.1 g/L on giant reed and cardoon hydrolysate, respectively. According to our previous work (Caporusso et al., 2023a), *L. tetrasporus* only began to take up xylose when the glucose concentration decreased to a level similar to that of the xylose concentration.

Tsigie et al. (2011) demonstrated that the transport system for D-xylose in *Y. lipolytica* is subjected to catabolite repression in the presence of hexose sugars. Although this aspect has not been studied in *L. tetrasporus*, presumably this yeast undergoes this effect. Furthermore, even if giant reed hydrolysate contained more sugar than the cardoon one, both microorganisms completely consumed all the sugars after 72 h.

Table 4 summarises the results of the batch-mode fermentation of giant reed and cardoon hydrolysates by the two oleaginous yeasts employed.

The intracellular lipid content was very similar (around 30 wt%) for the two yeasts grown on giant reed hydrolysate. In contrast, when cardoon hydrolysate was fermented, the value achieved by *L. starkeyi* was around 10 wt% lower than that achieved by *L. tetrasporus*. For both the yeasts, the starting lipid content was 10 wt%. At the end of the process, *L. starkeyi* reached a lipid content of 25.7 and 27.7 wt% on cardoon and giant reed hydrolysate, respectively. *L. tetrasporus* reached 35.6 and 29.5 wt% on cardoon and giant reed hydrolysate, respectively. A previous work reported a lipid content of 47 wt% for *L. tetrasporus* grown on a cardoon hydrolysate obtained by enzymatic catalysis, containing a higher sugars concentration (Caporusso et al., 2021). The difference in the achieved lipid content for *L. tetrasporus* was due to the different sugar concentrations (around 90 g/L comprising glucose and xylose) and the C/N weight ratio adopted during fermentation (C/N = 80 g/g). This ratio was double that in the present study, thus favouring lipogenesis. In the fermentation of giant reed hydrolysate, *L. starkeyi* converted 22 g/L of total reducing sugars into 3.0 g/L of lipids, achieving a lipid yield of 13.5 wt%, corresponding to around 50 wt% of the maximum theoretical yield (27.6 wt%) achievable for this yeast species from sugars. *L. tetrasporus* produced 15 % more lipids than *L. starkeyi,* producing about 3.6 g/L of lipids equal to a lipid yield of 16.0 wt%, corresponding to around 51 wt% of the maximum theoretical yield (31.6 wt%). In the fermentation of cardoon hydrolysate, about 18 g/L of total reducing sugars were converted by *L. starkeyi* into 2.6 g/L of lipids, achieving the lipid yield of 14.2 wt% (~52 wt% of the maximum value), while *L. tetrasporus* produced 3.3 g/L of lipids, equal to 17.6 wt% lipid yield (~56 wt% of the maximum theoretical yield). This last value represents the highest yield achieved in the experimental setup. Moreover, on both the hydrolysates, *L. tetrasporus* showed better lipogenic activity than *L. starkeyi*.

The literature reports that the experimental lipid yields achieved by *L. starkeyi* on synthetic and biomass-derived media range from 10 to 24 wt% (Jacob and Mathew, 2023). This attests to the values achieved in the present investigation being around 60 % of the maximum reported to date. In particular, when considering the fermentation of other types of lignocellulosic hydrolysate by the same yeast, Xavier et al. (2017) reported a lipid yield of 14.0 wt% when using sugarcane bagasse hydrolysate. Meanwhile, Kalam Azad (2014) claimed a lipid yield of 18.0 wt% using rice straw hydrolysate, and Calvey et al. (2016) obtained a yield of 14.0 wt% using corn stover hydrolysate.

Due to its recent isolation, only a few studies on *L. tetrasporus* are present in the scientific literature. Dien et al. (2016) reported oil yields of 10 and 14 wt% for the conversion of Douglas fir and switchgrass hydrolysates, respectively. Similarly, Chen et al. (2021) obtained a yield of 17 wt% by fermenting a switchgrass hydrolysate. These results are consistent with those obtained in the present study (Table 4).

Finally, the results obtained confirmed the feasibility of efficiently producing triglycerides from the cellulose fraction of giant reed and cardoon using *L. starkeyi* and *L. tetrasporus*.

3.4. Bioconversion of cardoon hemicellulose hydrolysate to lipids

The complete valorisation of lignocellulosic biomasses is challenging because exploiting the hemicellulose fraction is difficult. This is because most industrial microorganisms cannot assimilate pentose sugars, which are the main carbon source in hemicellulosic hydrolysates. To exploit all the carbohydrate components of the two selected lignocellulosic

Table 4
Fermentation results by *L. starkeyi* and *L. tetrasporus* on undetoxified giant reed hydrolysate and furfural-free cardoon hydrolysate.

Yeast	Culture medium	CS (g/L)	DCW (g/L)	L (g/L)	LC (wt%)	LY (wt%)	TLY[a] (wt%)	P (g/L/day)
L. starkeyi	Giant reed cellulose hydrolysate	22.2	10.8	3.0	27.7	13.5	48.9	1.0
	Cardoon cellulose hydrolysate	18.3	10.1	2.6	25.7	14.2	51.5	0.9
L. tetrasporus	Giant reed cellulose hydrolysate	22.4	12.2	3.6	29.5	16.0	50.6	1.2
	Cardoon cellulose hydrolysate	18.7	9.3	3.3	35.6	17.6	55.7	1.1

CS = consumed sugars; DCW = dry cell weight concentration; L = lipids concentration; LC = lipid content; LY = lipid yield; TLY = theoretical lipid yield; P = productivity.
[a] TLY = (LY/MTLY)*100, where the maximum theoretical lipids yield (MTLY) from sugars for *L. starkeyi* and *L. tetrasporus* is 27.6 and 31.6 wt%, respectively (Ratledge, 2014; Sutanto et al., 2018).

biomasses and thus increase the economic feasibility of the proposed cascade process, hemicellulose-derived monosaccharides were used as the sole carbon source for producing lipids by *L. starkeyi* and *L. tetrasporus*. The chemical composition of the hemicellulose hydrolysates obtained from giant reed and cardoon stalks was reported in Table 2. In a previous study (Di Fidio et al., 2021), the bioconversion of xylose and glucose derived from microwave-assisted $FeCl_3$-catalysed hydrolysis of raw giant reed hemicellulose to SCOs was optimised. Thus, in the present study, only the exploitation of the hemicellulose hydrolysate obtained by acid-catalysed steam explosion of cardoon stalks was investigated.

Moreover, the effect of pH on lipid accumulation by oleaginous yeasts was studied to favour the complete consumption of xylose. The pH value is an important parameter in microbial processes and is particularly crucial when using a lignocellulosic biomass hydrolysate as a growth medium, due to the low pH value intrinsic to the material caused by acidic pretreatment conditions (Amza et al., 2019; Brandenburg et al., 2016; Slininger et al., 2016). It has been observed that *L. starkeyi* can grow and accumulate lipids at low pH when cultured in synthetic media (Calvey et al., 2016). However, the behaviour of yeasts cultured in complex lignocellulosic hydrolysates must be studied, since these usually contain additional compounds such as organic acids (acetic acid, formic acid and levulinic acid), as well as aromatic and furanic derivatives, which could have different biochemical effects depending on the pH.

In the present study, the optimal pH value for *L. starkeyi* and *L. tetrasporus* was determined in order to increase both DCW production and oil accumulation. Three different pH values of cardoon hemicellulose hydrolysate were tested for each yeast, namely 4.5, 5.5, and 6.5.

Fig. 2 shows the kinetics of the fermentation processes of *L. starkeyi* (Figs. 2A and 2B) and *L. tetrasporus* (Figs. 2C and 2D) on hemicellulose hydrolysate at pH 5.5 (Figs. 2A and 2C) and 6.5 (Figs. 2B and 2D). Differently, significant cell growth was not observed for both yeasts at pH 4.5 (data not shown).

Both yeasts were able to grow using hemicellulose hydrolysate as the sole carbon source at pH levels of 5.5 and 6.5. While some previous studies have found that *L. starkeyi* is an acid-tolerant yeast capable of growing at pH 3.5 or lower on synthetic media (Calvey et al., 2016), the different chemical composition of undetoxified lignocellulosic hydrolysate must be considered, particularly the presence of organic acids in the medium, which are formed through homogeneous chemical catalysis. Indeed, at low pH, the proportion of undissociated organic acids (e.g. acetic, vanillic, levulinic and formic acids) increases. These acids can freely diffuse through the cell membrane and strongly inhibit yeast cells (Sugiyama et al., 2015).

As shown in Figs. 2A and 2B, *L. starkeyi* was able to grow on xylose-rich hydrolysate. However, unlike *L. tetrasporus*, it exhibited an initial latent phase during the first 24 h, followed by an exponential growth phase up to 72 h. Complete xylose conversion was observed, and the acetic acid concentration remained constant throughout the fermentation process. *L. tetrasporus* was able to detoxify the medium within the first 24 h (data not shown). As shown in Figs. 2C and 2D, no appreciable lag phase was observed, and xylose and acetic acid consumption started during the first day. Interestingly, acetic acid was consumed faster at pH 5.5 than at pH 6.5. Its concentration dropped to 0 g/L within 48 h at pH 5.5 and within 72 h at pH 6.5. Furthermore, the conversion of xylose to lipids also started within the first 24 h, which was different to the behaviour observed for the same yeast in the fermentation kinetics reported in Fig. 1. In this case, the negligible glucose concentration (0.9 g/L) in the hemicellulose hydrolysate (Table 2) favoured rapid xylose uptake and bioconversion.

Table 5 summarises the main outputs of the fermentation process as a function of both pH and yeast species.

Both yeasts exhibited the same trend, and lipid production was

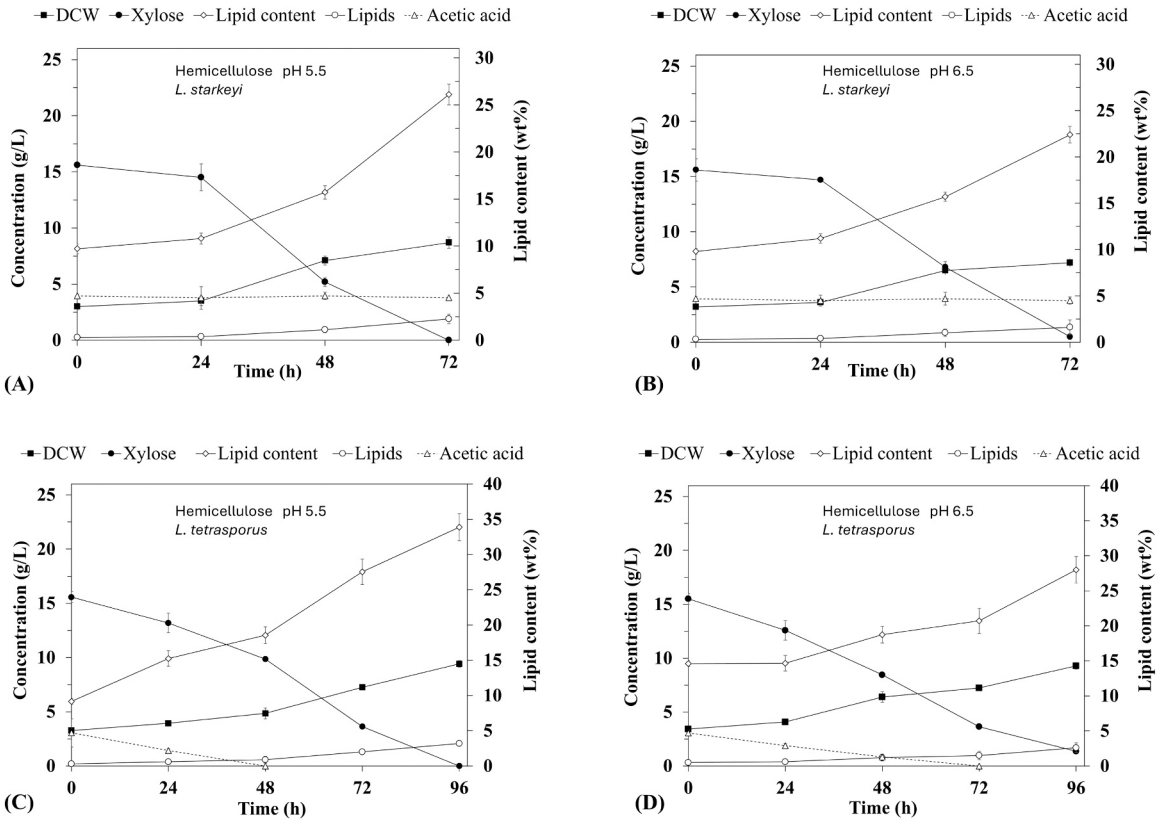

Fig. 2. Xylose concentration (g/L), acetic acid concentration (g/L), dry cell weight concentration (DCW, g/L), lipids concentration (g/L), and lipid content (wt%) as a function of process time during the cardoon hemicellulose hydrolysate fermentation at pH 5.5 (A, C) and 6.5 (B, D) by *L. starkeyi* (A, B) and *L. tetrasporus* (C, D).

Table 5
Fermentation results obtained by *L. starkeyi* and *L. tetrasporus* on cardoon hemicellulose hydrolysate at different pH values.

Yeast	pH	CS (g/L)	DCW (g/L)	L (g/L)	LC (wt%)	LY (wt%)	TLY[a] (wt%)	P (g/L/day)
L. starkeyi	6.5	16.0	7.2	1.6	22.4	10.0	36.2	0.5
	5.5	16.5	8.7	2.3	26.1	13.9	50.4	0.8
	4.5	-	-	-	-	-	-	-
L. tetrasporus	6.5	16.3	9.3	2.6	28.0	16.0	50.6	0.7
	5.5	16.5	9.4	3.2	33.9	19.4	61.4	0.8
	4.5	-	-	-	-	-	-	-

CS = consumed sugars; DCW = dry cell weight concentration; L = lipids concentration; LC = lipid content; LY = lipid yield; TLY = theoretical lipid yield; P = productivity.
[a] TLY = (LY/MTLY)*100, where the maximum theoretical lipids yield (MTLY) from sugars for *L. starkeyi* and *L. tetrasporus* is 27.6 and 31.6 wt%, respectively (Ratledge, 2014; Sutanto et al., 2018).

affected by pH. In particular, lipid production increased when the pH was decreased from 6.5 to 5.5; however, a further decrease to pH 4.5 prevented yeast growth. At pH 5.5, *L. starkeyi* achieved lipid yields and intracellular lipid contents of 14 and 26 wt%, respectively, which were approximately 15 % higher than the values obtained at pH 6.5 (10 and 22 wt%). Similarly, at the same pH, *L. tetrasporus* achieved a lipid yield and content of 19 and 34 wt%, respectively, 20 % higher than at pH 6.5 (16 and 28 wt%, respectively). Finally, *L. tetrasporus* exhibited 30 % higher lipid production than *L. starkeyi*, which can be attributed to its superior metabolic efficiency in converting xylose into triglycerides. Under the optimised process conditions, *L. starkeyi* achieved a theoretical lipid yield of 50.4 wt%, whereas *L. tetrasporus* reached a higher value of 61.4 wt%. Moreover, comparing the performance of each biocatalyst on cellulose and hemicellulose hydrolysates in terms of biomass growth, lipid content, yield and productivity (see Tables 4 and 5 for data) produced the same results for both yeasts. This confirms the feasibility of the proposed cascade and integrated biorefinery scheme for completely valorising the two selected lignocellulosic biomasses.

3.5. Chemical profile of long-chain fatty acid methyl esters from SCOs

Long-chain fatty acids methyl esters (FAMEs) were synthesised through a catalytic approach (described in Par. 2.9) starting from SCOs produced by *L. starkeyi* and *L. tetrasporus* on both cellulose and hemicellulose hydrolysates of giant reed and cardoon. These compounds represent a promising platform chemical in modern industrial chemistry as they can be used for a variety of commercial purposes, including the production of next-generation biodiesel (as a sustainable alternative to diesel derived from fossil fuels or edible oils), biosurfactants, biolubricants, chemicals, and other bio-based materials (Belousov et al., 2021; Biermann et al., 2021). Their applications are related to the chemical profile, which affects the main chemo-physical properties and reactivity. Table 6 shows the chemical profile of all the FAME mixtures produced in the present study from the SCOs obtained from the fermentation of different sugars-rich hydrolysates.

Yeast oils mostly consist of C16 and C18 fatty acids. The most abundant FAMEs were the esters of oleic acid (C18:1), palmitic acid (C16:0) and stearic acid (C18:0), accounting for around 90 % of the total composition for both yeasts. The remaining 10 % consists of the esters of palmitoleic acid (C16:1) and linoleic acid (C18:2), as well as traces of esters of shorter-chain acids such as lauric acid (C12:0) and myristic acid (C14:0), and longer-chain acids such as arachidic acid (C20:0), behenic acid (C22:0) and lignoceric acid (C24:0). Both yeasts exhibited a highly similar lipid profile across various hydrolysates. Furthermore, the different pH levels during the fermentation of cardoon hemicellulose hydrolysate did not significantly impact the FAME profile of either yeast. These results agreed with those reported in previous studies for the same oleaginous yeasts (Brandenburg et al., 2016; Dien et al., 2016; Pirozzi et al., 2015; Saha et al., 2024; Slininger et al., 2016). Pirozzi et al. (2015) obtained a very similar FAMEs profile for *L. starkeyi* grown on giant reed hydrolysate. Similarly, Brandenburg et al. (2016) obtained a similar lipid profile with *L. starkeyi* cultured on birch enzymatic hydrolysate. Although this is the first time that *L. tetrasporus* has been cultivated using hemicellulose hydrolysate, the resulting FAMEs profile was very similar to that obtained using cellulose hydrolysate in previous studies (Dien et al., 2016; Slininger et al., 2016). The high reproducibility of SCOs and FAMEs confirmed the biorefinery model's feasibility and robustness.

3.6. Levulinic and formic acids production from residual cellulose

This study implemented an innovative biorefinery process based on the synergistic combination of the chemical and biological conversion of two types of lignocellulosic biomass into various platform chemicals. Specifically, the final step of the cascade process involved the chemical treatment of giant reed and cardoon solid residues, obtained after the microwave-assisted $FeCl_3$-catalysed hydrolysis of cellulose to glucose, in the presence of the same inorganic salt. This produced levulinic acid and formic acid from residual and unconverted cellulose present in each biomass. The process was designed with a cascade model to meet the principles of the Circular Economy and Green Chemistry, significantly reducing waste production or outflow.

Levulinic acid and formic acid are two strategic platform chemicals in modern bio-based chemistry, as widely documented in the scientific

Table 6
Long-chain fatty acid methyl esters composition of the mixtures obtained from SCOs produced by *L. starkeyi* and *L. tetrasporus* starting from cellulose or hemicellulose hydrolysates.

Yeast	Medium	pH	Long-chain fatty acid methyl esters (%)				
			C16:0	C16:1	C18:0	C18:1	C18:2
L. starkeyi	Giant reed cellulose	5.5	36.7 ± 0.1	5.0 ± 0.2	17.1 ± 0.4	36.7 ± 0.7	4.5 ± 0.1
	Cardoon cellulose	5.5	36.8 ± 0.5	5.2 ± 0.2	16.9 ± 0.3	35.9 ± 0.5	5.2 ± 0.1
	Cardoon hemicellulose	5.5	35.5 ± 0.6	5.1 ± 0.1	14.4 ± 0.7	41.1 ± 0.3	3.9 ± 0.1
	Cardoon hemicellulose	6.5	35.9 ± 0.3	4.9 ± 0.1	15.3 ± 0.5	40.2 ± 0.1	3.7 ± 0.2
L. tetrasporus	Giant reed cellulose	5.5	33.6 ± 0.7	2.2 ± 0.1	19.4 ± 0.7	39.4 ± 0.8	1.5 ± 0.1
	Cardoon cellulose	5.5	38.0 ± 0.8	2.7 ± 0.1	22.0 ± 0.6	36.4 ± 0.5	2.4 ± 0.1
	Cardoon hemicellulose	5.5	31.1 ± 0.9	2.2 ± 0.1	20.6 ± 0.7	41.6 ± 0.9	1.3 ± 0.1
	Cardoon hemicellulose	6.5	33.5 ± 0.8	2.0 ± 0.1	21.3 ± 0.7	38.9 ± 0.9	1.3 ± 0.2

literature (Achour et al., 2023; Gérardy et al., 2020; Sajid et al., 2021). The same chemo-catalytic approach, based on the use of microwave irradiation coupled with $FeCl_3$ as a homogeneous and green catalyst, was adopted to produce levulinic acid and formic acid, but different reaction conditions were used with respect to those adopted in the saccharification step. In particular, relatively mild reaction conditions were used in glucose production (9 wt% biomass loading, 34 min, 2.7 wt% $FeCl_3$, 155 °C) to avoid the formation of by-products, such as furan derivatives. A solid residue containing cellulose (40 wt% for treated giant reed and 56 wt% for treated cardoon) and lignin (56 wt% for treated giant reed and 36 wt% for treated cardoon) was recovered from each biomass at this step. These solid residues were then hydrolysed using the previously optimised reaction conditions, namely biomass loading of 9 wt%, temperature of 190 °C, 2.4 wt% $FeCl_3$ and reaction time of 15 min (Di Fidio et al., 2020a). Under these reaction conditions, 87 % and 63 % of the residual glucan in giant reed and cardoon, respectively, were converted into levulinic and formic acids. Levulinic and formic acid yields of 64.5 and 86.7 mol%, respectively, were achieved for the giant reed residue. Yield values of 63.4 and 81.4 mol% were obtained for the cardoon residue, respectively. These results were significantly higher than those previously reported in the literature (Zheng et al., 2017), confirming the beneficial effect of the cascade valorisation of the cellulose fraction of both lignocellulosic biomasses.

3.7. Cascade process mass balance

Fig. 3 shows the mass balance flow diagram of the entire cascade biorefinery process, which was designed and developed in this study to enable the full exploitation of giant reed.

Starting from 100 g of the dry biomass, a first selective fractionation and hydrolysis of the hemicellulose was performed as described in a previous study (Di Fidio et al., 2021), obtaining a liquid fraction mainly rich in xylose and glucose. Using 0.84 g of $FeCl_3{\cdot}6\,H_2O$ for 3 g of biomass corresponds to using approximately 0.50 g of $FeCl_3$, which is the effective catalyst involved in the hydrolysis reaction mechanism. Furthermore, the catalyst/biomass weight ratio of 0.17 is comparable to, or even lower than, values reported in the literature for similar hydrolysis reactions. For example, Kamireddy et al. (2013) used 20.3 g of $FeCl_3$ for 105 g of unpretreated corn stover, giving a catalyst/biomass weight ratio of 0.19 wt/wt. Similarly, López-Linares et al. (2013) used 42.2 g of $FeCl_3$ for 120 g of unpretreated olive tree biomass, giving a catalyst/biomass weight ratio of 0.35 wt/wt, and Marcotullio et al. (2011) used 16.2 g of $FeCl_3$ for 100 g of unpretreated wheat straw, giving a catalyst/biomass weight ratio of 0.16 wt/wt. The catalyst can also be recycled. Metal chlorides can be recovered as metal hydroxides by ultrafiltration and subsequently regenerated by acid treatment (e.g., HCl), enabling their reuse in the process. This allows the catalyst to be recycled and reused in the process (Kamireddy et al., 2013; Loow et al., 2015).

This hydrolysate was used as an undetoxified culture medium to produce 4.7 g of SCO by the yeast *L. starkeyi*. The cellulose-rich solid fraction was used as substrate to produce a glucose-rich hydrolysate in the second step. The latter was used as an undetoxified fermentation medium for the growth of the two oleaginous yeasts, obtaining 1.7 and 2.1 g of SCOs by *L. starkeyi* and *L. tetrasporus*, respectively.

In the third step, the solid residue obtained from the saccharification step was used as substrate for the catalytic production of 6.0 g levulinic acid and 3.2 g formic acid. The final solid residue obtained at the end of the process, representing around 20 wt% of the starting biomass, was composed of 85.3 wt% lignin and 8 wt% cellulose on dry matter. This lignin-rich material has the potential to be used in the production of bio-based materials, such as lignin-derived aromatics, microporous activated carbons for the adsorption of gaseous or liquid pollutants, and bio-based composite materials and/or biofuels, including pyrolysis oil and syngas. This would allow the complete valorisation of the initial lignocellulosic biomass.

Fig. 4 shows the mass balance flow diagram of the slightly different biorefinery implemented in the present work for the complete valorisation of cardoon stalks.

Also in this case, starting from 100 g of dry biomass, liquid and solid fractions were obtained after the acid-catalysed steam explosion pretreatment aiming at selectively hydrolyse the hemicellulose fraction and deconstruct the three-dimensional lignocellulosic matrix. From this first step, approximately 70 wt% of the xylan was converted to xylose. The undetoxified liquid fraction was then fermented, under the optimised reaction conditions previously described, by *L. starkeyi* and *L. tetrasporus*, obtaining 1.4 and 1.9 g of triglycerides, respectively. The pretreated solid fraction was then subjected to the saccharification process in the second step. To minimise the formation of toxic by-products, mild reaction conditions were adopted, reaching a glucose yield of around 30 mol% with respect to the moles of glucan in the substrate. In this way, the obtained glucose-rich hydrolysate was fermented by the two oleaginous yeasts, achieving 1.3 and 1.6 g of SCOs by *L. starkeyi* and *L. tetrasporus*, respectively. In the third process step, the solid residue deriving from the saccharification process was used as a substrate for the chemical production of levulinic and formic acids, obtaining 11.4 and 5.8 g, respectively.

By comparing the best scenarios of the two biorefinery models, it was found that from 100 g of dry giant reed, 6.8 g of triglycerides, 6.0 g of levulinic acid, 3.2 g of formic acid, and 21.1 g of lignin could be obtained. Meanwhile, from 100 g of dry cardoon stalks, the production was 3.5 g of triglycerides, 11.4 g of levulinic acid, 5.8 g of formic acid, and 25.1 g of lignin. In both cases, the complete and tailored exploitation of the starting materials was successfully implemented from the perspective of Green Chemistry and the Circular Economy. Furthermore, these data provide a foundation for future studies that integrate data-driven approaches. In these studies, machine learning could optimise reaction parameters and predict conversion yields across a range of different types of biomasses (Qiao et al., 2025). This would improve the efficiency and the economic sustainability of multi-product cascade biorefineries. This study proposes an innovative and versatile catalytic route for biomass saccharification using the low-cost homogeneous catalyst $FeCl_3$ as an alternative to costly enzymatic processes. Therefore, the choice of catalytic strategies for scaling up the process should be based on a comprehensive LCA study, which is beyond the scope of this work.

4. Conclusions

In the present study, for the first time, two innovative cascade biorefinery schemes were developed to completely valorise two lignocellulosic biomasses, namely cardoon stalks and giant reed, by a synergistic combination of chemical and biological catalysis. In particular, for both the biomasses, a first treatment was implemented to selectively hydrolyse the hemicellulose fraction to give mainly xylose in the liquid fraction, reducing the formation of inhibitor compounds, such as 5-hydroxymethylfurfural and furfural. This goal was reached by a microwave-assisted $FeCl_3$-catalysed hydrolysis for giant reed and H_2SO_4-catalysed steam explosion for cardoon stalks. The xylose-rich hydrolysate was then used as culture medium for the biological conversion of sugars to triglycerides by the two promising yeasts *L. starkeyi* and *L. tetrasporus*. The cellulose-rich solid fraction was then subjected to the saccharification step to give glucose by adopting the microwave-assisted $FeCl_3$ catalysis under different reaction conditions, in order to maximise the production of glucose and minimise the formation of toxic compounds for the yeast's growth. The glucose-rich hydrolysates obtained for the two biomasses were used as fermentation media in the presence of the same yeasts to produce new-generation oils, which were then used to produce long-chain fatty acid methyl esters (*i.e.* biodiesel). In the last step, the solid residue deriving from the saccharification step was used as substrate to valorise the unconverted cellulose by producing levulinic and formic acids through the same chemical catalytic approach

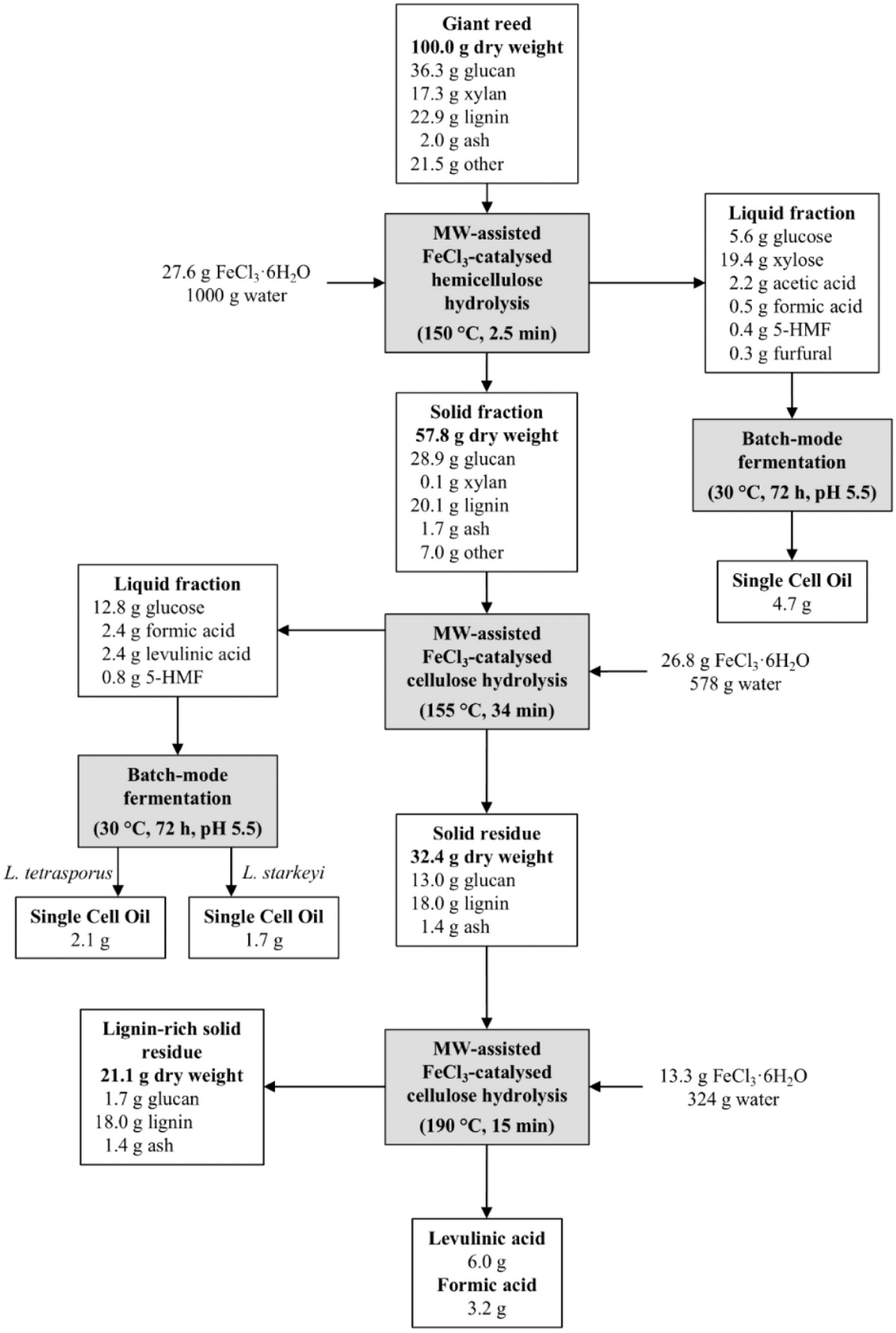

Fig. 3. Mass balance flow diagram of the cascade biorefinery process developed for the complete exploitation of giant reed to give different added-value bioproducts.

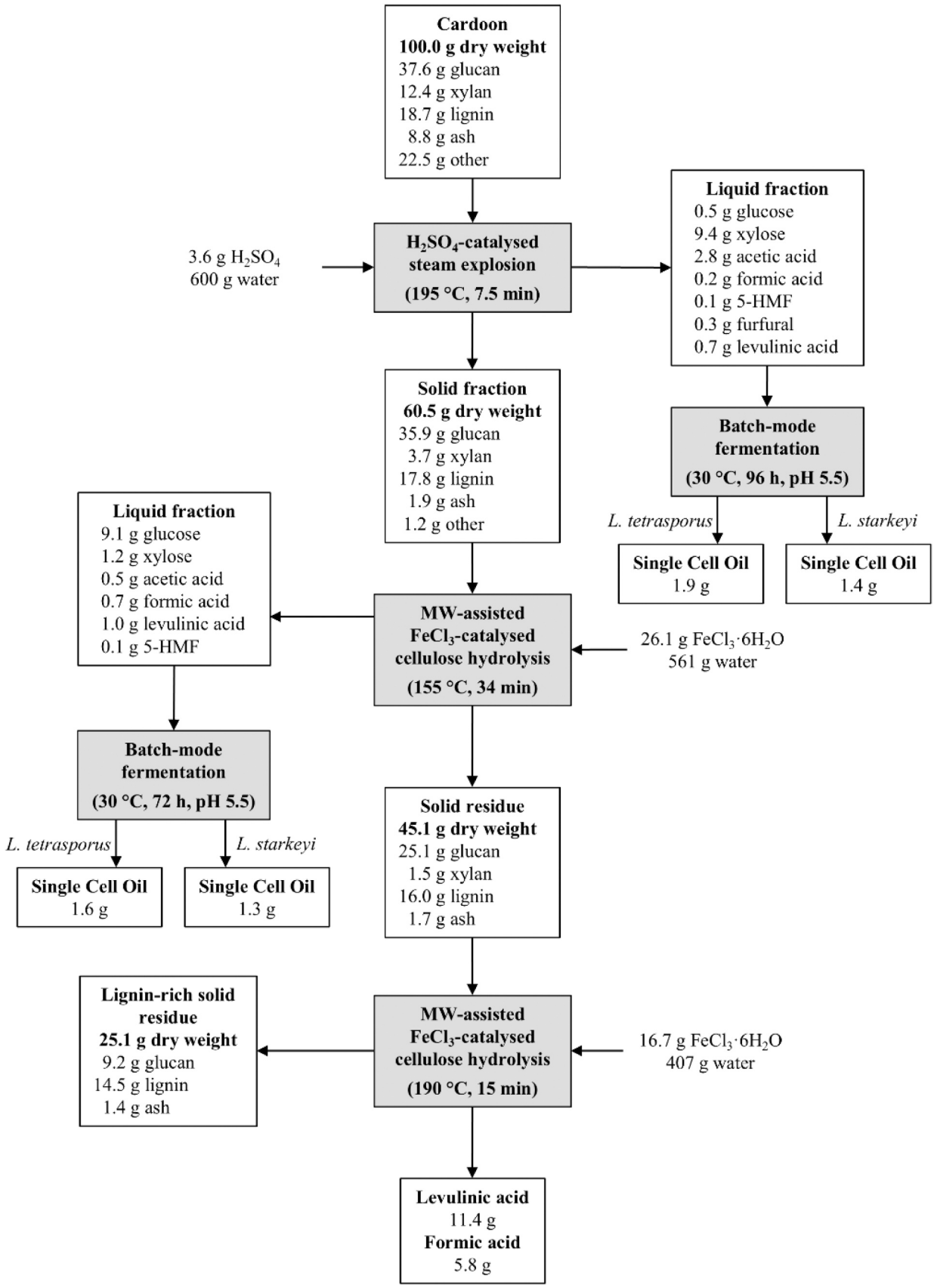

Fig. 4. Mass balance flow diagram of the cascade biorefinery process developed for the complete exploitation of cardoon stalks to give different added-value bioproducts.

but under different reaction conditions. The final solid residue was mainly composed of lignin, which could be potentially exploited by further chemical or biological routes from the perspective of Green Chemistry and Circular Economy.

CRediT authorship contribution statement

Federico Liuzzi: Writing – review & editing, Validation, Formal analysis. **Egidio Viola:** Writing – review & editing, Supervision. **Isabella De Bari:** Writing – review & editing, Supervision, Conceptualization. **Antonio Caporusso:** Writing – original draft, Validation, Methodology, Formal analysis, Conceptualization. **Nicola Di Fidio:** Writing – original draft, Methodology, Formal analysis, Conceptualization.

Declaration of Competing Interest

The authors declare that there are no conflicts of interest.

Acknowledgements

N.D.F. thanks the colleagues of ENEA Trisaia Research Centre for the hospitality in their laboratories.

Data availability

Data will be made available on request.

References

Achour, M., Álvarez-Hernández, D., Ruiz-López, E., Megías-Sayago, C., Ammari, F., Ivanova, S., Centeno, M.Á., 2023. Formic acid as renewable reagent and product in biomass upgrading. Tetrahedron Green. Chem. 2, 100020. https://doi.org/10.1016/j.tgchem.2023.100020.

Amza, R.L., Kahar, P., Juanssilfero, A.B., Miyamoto, N., Otsuka, H., Kihira, C., Ogino, C., Kondo, A., 2019. High cell density cultivation of *Lipomyces starkeyi* for achieving highly efficient lipid production from sugar under low C/N ratio. Biochem. Eng. J. 149, 107236. https://doi.org/10.1016/j.bej.2019.05.013.

Belousov, A.S., Esipovich, A.L., Kanakov, E.A., Otopkova, K.V., 2021. Recent advances in sustainable production and catalytic transformations of fatty acid methyl esters. Sustain. Energy Fuels 5, 4512–4545. https://doi.org/10.1039/d1se00830g.

Biermann, U., Bornscheuer, U.T., Feussner, I., Meier, M.A.R., Metzger, J.O., 2021. Fatty acids and their derivatives as renewable platform molecules for the chemical industry. Angew. Chem. Int. Ed. 60, 20144–20165. https://doi.org/10.1002/anie.202100778.

Brandenburg, J., Blomqvist, J., Pickova, J., Bonturi, N., Sandgren, M., Passoth, V., 2016. Lipid production from hemicellulose with *Lipomyces starkeyi* in a pH regulated fed-batch cultivation. Yeast 33, 451–462. https://doi.org/10.1002/yea.3160.

Calvey, C.H., Su, Y.K., Willis, L.B., McGee, M., Jeffries, T.W., 2016. Nitrogen limitation, oxygen limitation, and lipid accumulation in *Lipomyces starkeyi*. Bioresour. Technol. 200, 780–788. https://doi.org/10.1016/j.biortech.2015.10.104.

Caporusso, A., De Bari, I., Valerio, V., Albergo, R., Liuzzi, F., 2021. Conversion of cardoon crop residues into single cell oils by *Lipomyces tetrasporus* and *Cutaneotrichosporon curvatus*: process optimizations to overcome the microbial inhibition of lignocellulosic hydrolysates. Ind. Crops Prod. 159, 113030. https://doi.org/10.1016/j.indcrop.2020.113030.

Caporusso, A., Giuliano, A., Liuzzi, F., Barletta, D., De Bari, I., 2023b. Techno-economic analysis of green diesel production process from vegetable oils. Chem. Eng. Trans. 100, 13–18. https://doi.org/10.3303/CET23100003.

Caporusso, A., De Bari, I., Giuliano, A., Liuzzi, F., Albergo, R., Pietrafesa, R., Siesto, G., Romanelli, A., Braccio, G., Capece, A., 2023a. Optimization of wheat straw conversion into microbial lipids by *Lipomyces tetrasporus* DSM 70314 from bench to pilot scale. Fermentation 9, 180. https://doi.org/10.3390/fermentation9020180.

Caporusso, A., Casiello, M., Leo, V.De, Perna, A., Catucci, L., Accolti, L.D., Capece, A., De Bari, I., 2025. Low impact methods for microbial lipids production for third generation biofuels and biobased polyurethanes. J. Environ. Chem. Eng. 13, 117375. https://doi.org/10.1016/j.jece.2025.117375.

Chen, J., Wang, X., Zhang, B., Yang, Y., Song, Y., Zhang, F., Liu, B., Zhou, Y., Yi, Y., Shan, Y., Lü, X., 2021. Integrating enzymatic hydrolysis into subcritical water pretreatment optimization for bioethanol production from wheat straw. Sci. Total Environ. 770, 145321. https://doi.org/10.1016/j.scitotenv.2021.145321.

Chen, Z., Sun, X., Sun, Y., Wan, C., 2021. Efficient biosynthesis of lipids from concentrated biomass hydrolysates by an oleaginous yeast. Bioresour. Technol. Rep. 15, 100712. https://doi.org/10.1016/J.BITEB.2021.100712.

D'Orsi, R., Di Fidio, N., Antonetti, C., Raspolli Galletti, A.M., Operamolla, A., 2023. Isolation of Pure Lignin and Highly Digestible Cellulose from Defatted and Steam-Exploded *Cynara cardunculus*. ACS Sustain. Chem. Eng. 11, 1875–1887. https://doi.org/10.1021/acssuschemeng.2c06356.

De Bari, I., Giuliano, A., Petrone, M.T., Stoppiello, G., Fatta, V., Giardi, C., Razza, F., Novelli, A., 2020. From cardoon lignocellulosic biomass to bio-1,4 butanediol: An integrated biorefinery model. Processes 8, 1585. https://doi.org/10.3390/pr8121585.

Di Fidio, N., Antonetti, C., Raspolli Galletti, A.M., 2019. Microwave-assisted cascade exploitation of giant reed (*Arundo donax* L.) to xylose and levulinic acid catalysed by ferric chloride. Bioresour. Technol. 293, 122050. https://doi.org/10.1016/j.biortech.2019.122050.

Di Fidio, N., Raspolli Galletti, A.M., Fulignati, S., Licursi, D., Liuzzi, F., De Bari, I., Antonetti, C., 2020b. Multi-step exploitation of raw *Arundo donax* L. for the selective synthesis of second-generation sugars by chemical and biological route. Catalysts 10, 79. https://doi.org/10.3390/catal10010079.

Di Fidio, N., Fulignati, S., De Bari, I., Antonetti, C., Raspolli Galletti, A.M., 2020a. Optimisation of glucose and levulinic acid production from the cellulose fraction of giant reed (*Arundo donax* L.) performed in the presence of ferric chloride under microwave heating. Bioresour. Technol. 313, 123650. https://doi.org/10.1016/j.biortech.2020.123650.

Di Fidio, N., Ragaglini, G., Dragoni, F., Antonetti, C., Raspolli Galletti, A.M., 2021. Integrated cascade biorefinery processes for the production of single cell oil by *Lipomyces starkeyi* from *Arundo donax* L. hydrolysates. Bioresour. Technol. 325, 124635. https://doi.org/10.1016/j.biortech.2020.124635.

Dien, B.S., Zhu, J.Y., Slininger, P.J., Kurtzman, C.P., Moser, B.R., O'Bryan, P.J., Gleisner, R., Cotta, M.A., 2016. Conversion of SPORL pretreated Douglas fir forest residues into microbial lipids with oleaginous yeasts. RSC Adv. 6, 20695–20705. https://doi.org/10.1039/c5ra24430g.

Efrinalia, W., Novia, N., Melwita, E., 2022. Kinetic Model for Enzymatic Hydrolysis of Cellulose from Pre-Treated Rice Husks. Fermentation 8, 417. https://doi.org/10.3390/fermentation8090417.

Fabbrizi, G., Giannoni, T., Lorenzi, L., Nicolini, A., Iodice, P., Coccia, V., Cavalaglio, G., Gelosia, M., 2022. High solid and low cellulase enzymatic hydrolysis of cardoon stems pretreated by acidified γ-valerolactone/water solution. Energies 15, 2600. https://doi.org/10.3390/en15072600.

Fernandes, M.C., Ferro, M.D., Paulino, A.F.C., Chaves, H.T., Evtuguin, D.V., Xavier, A.M.R.B., 2018. Comparative study on hydrolysis and bioethanol production from cardoon and rockrose pretreated by dilute acid hydrolysis. Ind. Crops Prod. 111, 633–641. https://doi.org/10.1016/j.indcrop.2017.11.037.

Gallego-García, M., Susmozas, A., Moreno, A.D., Negro, M.J., 2022. Evaluation and identification of key economic bottlenecks for cost-effective microbial oil production from fruit and vegetable residues. Fermentation 8, 334. https://doi.org/10.3390/fermentation8070334.

Gérardy, R., Debecker, D.P., Estager, J., Luis, P., Monbaliu, J.C.M., 2020. Continuous flow upgrading of selected C2-C6 platform chemicals derived from biomass. Chem. Rev. 120, 7219–7347. https://doi.org/10.1021/acs.chemrev.9b00846.

Hernández-Mendoza, A.G., Saldaña-Trinidad, S., Martínez-Hernández, S., Pérez-Sariñana, B.Y., Láinez, M., 2021. Optimization of alkaline pretreatment and enzymatic hydrolysis of cocoa pod husk (*Theobroma cacao* L.) for ethanol production. Biomass.. Bioenergy 154, 106268. https://doi.org/10.1016/j.biombioe.2021.106268.

Jacob, A., Mathew, J., 2023. Recent advances in using *Lipomyces starkeyi* for the production of single-cell oil. J. Pure Appl. Microbiol 17, 693–704. https://doi.org/10.22207/JPAM.17.2.06.

Kalam Azad, A., 2014. Production of microbial lipids from rice straw hydrolysates by *Lipomyces starkeyi* for biodiesel synthesis. J. Microb. Biochem. Technol. s8. https://doi.org/10.4172/1948-5948.s8-008.

Kamireddy, S.R., Li, J., Tucker, M., Degenstein, J., Ji, Y., 2013. Effects and mechanism of metal chloride salts on pretreatment and enzymatic digestibility of corn stover. Ind. Eng. Chem. Res. 52, 1775–1782. https://doi.org/10.1021/ie3019609.

Keramidas, K., Fosse, F., Diaz-Vazques, A., Schade, B., Tchung-Ming, S., Weitzel, M., Vandyck, T., Wojtowicz, K., 2021. Global energy and climate outlook 2020: a new normal beyond covid-19. Publ. Off. Eur. Union. https://doi.org/10.2760/608429.

Kobayashi, T., Nakajima, L., 2021. Sustainable development goals for advanced materials provided by industrial wastes and biomass sources. Curr. Opin. Green. Sustain. Chem. 28, 100439. https://doi.org/10.1016/j.cogsc.2020.100439.

Kumar, K.K., Deeba, F., Pandey, A.K., Islam, A., Paul, D., Gaur, N.A., 2025. Sustainable lipid production by oleaginous yeasts: current outlook and challenges. Bioresour. Technol. 421, 132205. https://doi.org/10.1016/J.BIORTECH.2025.132205.

Lemões, J.S., Lemons e Silva, C.F., Avila, S.P.F., Montero, C.R.S., Silva, S.D., Samios, D., Peralba, C.R., 2018. Chemical pretreatment of *Arundo donax* L. for second-generation ethanol production. Electron. J. Biotechnol. 31, 67–74. https://doi.org/10.1016/j.ejbt.2017.10.011.

Loow, Y.L., Wu, T.Y., Tan, K.A., Lim, Y.S., Siow, L.F., Jahim, J.M., Mohammad, A.W., Teoh, W.H., 2015. Recent advances in the application of inorganic salt pretreatment for transforming lignocellulosic biomass into reducing sugars. J. Agric. Food Chem. 63, 8349–8363. https://doi.org/10.1021/acs.jafc.5b01813.

López-Linares, J.C., Romero, I., Moya, M., Cara, C., Ruiz, E., Castro, E., 2013. Pretreatment of olive tree biomass with $FeCl_3$ prior enzymatic hydrolysis. Bioresour. Technol. 128, 180–187. https://doi.org/10.1016/j.biortech.2012.10.076.

Madadi, M., Elsayed, M., Song, G., Shafiei-Alavijeh, R., Denayer, J.F.M., Kargaran, E., Azad, S., Al, Karimi, K., Sun, F., Gupta, V.K., 2025. Transformative biorefinery model for biomass valorization into biofuel and renewable platform chemicals. J. Energy Chem. 110, 109–123. https://doi.org/10.1016/J.JECHEM.2025.06.016.

Madian, H.R., Hamouda, H.I., Hosny, M., 2022. Statistical optimization of bioethanol production from giant reed hydrolysate by *Candida tropicalis* using Taguchi design. J. Biotechnol. 360, 71–78. https://doi.org/10.1016/j.jbiotec.2022.10.007.

Mandim, F., Santos-Buelga, C., Ferreira, I., Petropoulos, S.A., Barros, L., 2023. The wide spectrum of industrial applications for cultivated cardoon (*Cynara cardunculus* L. var. Altilis DC): A review. Food Chem. 423, 136275. https://doi.org/10.1016/J.FOODCHEM.2023.136275.

Marcotullio, G., Krisanti, E., Giuntoli, J., De Jong, W., 2011. Selective production of hemicellulose-derived carbohydrates from wheat straw using dilute HCl or $FeCl_3$ solutions under mild conditions. X-ray and thermo-gravimetric analysis of the solid residues. Bioresour. Technol. 102, 5917–5923. https://doi.org/10.1016/j.biortech.2011.02.092.

Mota, M.N., Múgica, P., Sá-Correia, I., 2022. Exploring yeast diversity to produce lipid-based biofuels from agro-forestry and industrial organic residues. J. Fungi 8, 687. https://doi.org/10.3390/jof8070687.

Ortega, Z., Bolaji, I., Suárez, L., Cunningham, E., 2024. A review of the use of giant reed (*Arundo donax* L.) in the biorefineries context. Rev. Chem. Eng. 40, 305–328. https://doi.org/10.1515/revce-2022-0069.

Pirozzi, D., Fiorentino, N., Impagliazzo, A., Sannino, F., Yousuf, A., Zuccaro, G., Fagnano, M., 2015. Lipid production from *Arundo donax* grown under different agronomical conditions. Renew. Energy 77, 456–462. https://doi.org/10.1016/j.renene.2014.12.046.

Pizzimenti, S., Bernazzani, L., Tinè, M.R., Duce, C., Bonaduce, I., 2022. Unravelling the effect of carbon black in the autoxidation mechanism of polyunsaturated oils. J. Therm. Anal. Calor. 147, 5451–5462. https://doi.org/10.1007/s10973-021-11165-8.

Qiao, Y., Kargaran, E., Ji, H., Madadi, M., Rafieyan, S., Liu, D., 2025. Data-driven insights for enhanced cellulose conversion to 5-hydroxymethylfurfural using machine learning. Bioresour. Technol. 430, 132582. https://doi.org/10.1016/J.BIORTECH.2025.132582.

Ratledge, C., 2014. The role of malic enzyme as the provider of NADPH in oleaginous microorganisms: a reappraisal and unsolved problems. Biotechnol. Lett. 36, 1557–15568. https://doi.org/10.1007/s10529-014-1532-3.

Saha, S., Laha, D., Mandal, E., Datta, D., Das, B., Jeon, B.H., 2024. The potency of oleaginous yeast *Lipomyces starkeyi* in organic waste valorization to biodiesel. Energy Environ. 36, 2131–2151. https://doi.org/10.1177/0958305X241292285.

Sajid, M., Farooq, U., Bary, G., Azim, M.M., Zhao, X., 2021. Sustainable production of levulinic acid and its derivatives for fuel additives and chemicals: progress, challenges, and prospects. Green. Chem. 23, 9198–9238. https://doi.org/10.1039/d1gc02919c.

Slininger, P.J., Dien, B.S., Kurtzman, C.P., Moser, B.R., Bakota, E.L., Thompson, S.R., O'Bryan, P.J., Cotta, M.A., Balan, V., Jin, M., Sousa, L., da, C., Dale, B.E., 2016. Comparative lipid production by oleaginous yeasts in hydrolyzates of lignocellulosic biomass and process strategy for high titers. Biotechnol. Bioeng. 113, 1676–1690. https://doi.org/10.1002/bit.25928.

Sluiter, A., Ruiz, R.O., Scarlata, C., Sluiter, J., Templeton, D., 2004b. Determination of extractives in biomass. Biomass.. Anal. Technol. Team Lab. Anal. Proced. Tech. Rep. NREL/TP-510-42619. https://doi.org/2008.

Sluiter, A., Hames, B., Ruiz, R.O., Scarlata, C., Sluiter, J., Templeton, D., 2004a. Determination of Ash in Biomass, Biomass Analysis Technology Team Laboratory Analytical Procedure. NREL, pp. 1–6 https://doi.org/TP-510-42622.

Sluiter, A., Hames, B., Ruiz, R., Slui, C.S., Templeton, D., Crocker, D., 2008. Determination of Structural Carbohydrates and Lignin in Biomass: Laboratory Analytical Procedure (LAP). Tech. Rep. NREL/TP-510-42618, 1617, 1-16.

Sluiter, A., Hames, B., Hyman, D., Payne, C., Ruiz, R., Scarlata, C., Sluiter, J., Templeton, D., Wolfe, J., 2008b. Determination of total solids in biomass and total dissolved solids in liquid process samples, 9. National Renewable Energy Laboratory (NREL), pp. 1–6. NREL/TP-510-42621.

Sugiyama, M., Sasano, Y., Harashima, S., 2015. Mechanism of yeast adaptation to weak organic acid stress, in: Stress Biology of Yeasts and Fungi: Applications for Industrial Brewing and Fermentation. https://doi.org/10.1007/978-4-431-55248-2_7.

Sutanto, S., Zullaikah, S., Tran-Nguyen, P.L., Ismadji, S., Ju, Y.H., 2018. *Lipomyces starkeyi*: Its current status as a potential oil producer. Fuel Process. Technol. 177, 39–55. https://doi.org/10.1016/j.fuproc.2018.04.012.

Szczepańska, P., Hapeta, P., Lazar, Z., 2022. Advances in production of high-value lipids by oleaginous yeasts. Crit. Rev. Biotechnol. 42, 1–22. https://doi.org/10.1080/07388551.2021.1922353.

Taheripour, F., Sajedinia, E., Karami, O., 2022. Oilseed Cover Crops for Sustainable Aviation Fuels Production and Reduction in Greenhouse Gas Emissions Through Land Use Savings. Front. Energy Res. 9. https://doi.org/10.3389/fenrg.2021.790421.

Tan, Y., Madadi, M., Song, G., Sun, C., Elsayed, M., Sun, F., Gupta, V.K., 2025. Integrated biorefinery routes to transform furfural waste into 2G biofuels and PFOA-adsorbing biochar. Green. Chem. 27, 3573–3589. https://doi.org/10.1039/d5gc00199d.

Tsigie, Y.A., Wang, C.Y., Truong, C.T., Ju, Y.H., 2011. Lipid production from *Yarrowia lipolytica* Po1g grown in sugarcane bagasse hydrolysate. Bioresour. Technol. 102, 9216–9222. https://doi.org/10.1016/j.biortech.2011.06.047.

Wang, Q., Guo, F.J., Rong, Y.J., Chi, Z.M., 2012. Lipid production from hydrolysate of cassava starch by *Rhodosporidium toruloides* 21167 for biodiesel making. Renew. Energy 46, 164–168. https://doi.org/10.1016/j.renene.2012.03.002.

Xavier, M.C.A., Coradini, A.L.V., Deckmann, A.C., Franco, T.T., 2017. Lipid production from hemicellulose hydrolysate and acetic acid by *Lipomyces starkeyi* and the ability of yeast to metabolize inhibitors. Biochem. Eng. J. 118, 11–19. https://doi.org/10.1016/j.bej.2016.11.007.

Yildirim, O., Tunay, D., Ozkaya, B., 2023. Optimization of enzymatic hydrolysis conditions of chemical pretreated cotton stalk using response surface methodology for enhanced bioethanol production yield. Biomass.. Convers. Biorefinery 13, 6623–6634. https://doi.org/10.1007/s13399-021-01692-7.

Zhang, L., Lee, J.T.E., Ok, Y.S., Dai, Y., Tong, Y.W., 2022. Enhancing microbial lipids yield for biodiesel production by oleaginous yeast *Lipomyces starkeyi* fermentation: a review. Bioresour. Technol. 344, 126294. https://doi.org/10.1016/j.biortech.2021.126294.

Zheng, X., Zhi, Z., Gu, X., Li, X., Zhang, R., Lu, X., 2017. Kinetic study of levulinic acid production from corn stalk at mild temperature using $FeCl_3$ as catalyst. Fuel 187, 261–267. https://doi.org/10.1016/j.fuel.2016.09.019.